# Experimental investigation of the diameter and length effects of the dendritic, bottomless, extended structure on reservoir sediment removal efficiency by flushing

**Article** *in* Journal of Hydro-environment Research · September 2022

DOI: 10.1016/j.jher.2022.09.002

CITATIONS
3

READS
143

**5 authors**, including:

Hadi Haghjouei
Shahid Bahonar University of Kerman
**6** PUBLICATIONS **14** CITATIONS
SEE PROFILE

Majid Rahimpour
Shahid Bahonar University of Kerman
**36** PUBLICATIONS **281** CITATIONS
SEE PROFILE

Kourosh Qaderi
Shahid Bahonar University of Kerman
**58** PUBLICATIONS **602** CITATIONS
SEE PROFILE

Sameh Ahmed Kantoush
Kyoto University
**191** PUBLICATIONS **1,893** CITATIONS
SEE PROFILE

New Journal and we have not received input yet 45 (2022) 15–28

Contents lists available at ScienceDirect

Journal of Hydro-environment Research

journal homepage: www.elsevier.com/locate/jher

Research papers

# Experimental investigation of the diameter and length effects of the dendritic, bottomless, extended structure on reservoir sediment removal efficiency by flushing

Hadi Haghjouei [a,*], Majid Rahimpour [a], Kourosh Qaderi [a], Sameh A. Kantoush [b], Sepideh Beiramipour [a]

[a] Department of Water Engineering, Shahid Bahonar University of Kerman, Kerman, Iran
[b] Disaster Prevention Research Institute, Kyoto University, Japan

ARTICLE INFO

*Keywords:*
Pressurized flushing
Sediment removal efficiency
Sediment flushing cone
Dendritic bottomless extended structure

ABSTRACT

Sedimentation in front of a dam is the main obstacle against reservoir sustainability. Due to the limited availability of suitable new dam sites, the ramifications of inefficient sediment management are associated with socio-economic concerns and environmental issues. Most of the existing sediment management techniques are unfavorable for arid and semi-arid regions due to their impacts on available water storage and power generation. Therefore, pressure flushing is an economical desilting method as it releases little water through the bottom outlet. However, one of the main disadvantages of pressurized flushing is limited sediment removal near the bottom outlet. In this paper, the impacts of a dendritic, bottomless, and extended (DBE) structure were investigated to develop the scour cone to a broader area. Several experiments were carried out with four different diameters (125, 160, 200, and 250 mm), four different lengths (30, 50, 80, and 110 cm), and three discharge rates (12.5, 15, and 18 L/s), to identify the dimensions of the extended structure with the most efficient operation. The results indicated that the DBE structure with a length dimensionless index of $L_{DBE}/D_o = 10$, a diameter dimensionless index of $D_{DBE}/D_o = 1.14$, and an outflow discharge dimensionless index of $Fr_o = 1.82$, yielded a 36.55-fold increase in the sediment flushing cone dimensions and sediment removal efficiency compared to a reference test. Finally, a dimensionless equation is presented for calculating the sediment flushing cone dimensions, according to a statistical analysis of the results. Two diagrams are provided to illustrate the interrelationship between the distance limits of scour, length, and diameter of the structure and outlet discharges.

## 1. Introduction

Over the last 30 years, water storage capacity has been reducing worldwide owing to reservoir sedimentation faster than new reservoirs are being built, threatening the availability of storage (Randle et al., 2019). The rate of reduction in capacity is 1–2 % per year globally (Isaac and Eldho, 2019). However, it is much higher in such regions as Asia, with the highest average annual rate in the world being 2.3 % in China (Cao et al., 2019). Sedimentation eventually decreases reservoir capacity and has adverse operational and economic effects on dam functions such as water supply and power generation (Ballio and Tait, 2012; White, 2001). An increase in groundwater level and a decrease in the natural capacity to control flood and water diversion or retreat adversely impact sedimentation in the dam upstream (Tigrek et al., 2009).

Various methods have controlled reservoir sedimentation, each with specific constraints and effects. Sediment management techniques are usually classified into four groups (Morris and Fan, 2009; Morris, 2015; Sumi and Kantoush, 2010), namely 1) decreasing sediment entry from upstream by trapping the sediment above the reservoir, 2) determining the route of sediments to minimize their accumulation, by sediment bypass and reservoir sluicing, 3) removing trapped sediments by dry excavation, dredging, hydrosuction, and hydraulic flushing, and 4) using adaptive methods such as reallocating storage and modifying intake. In the case of constructed dam reservoirs, accumulated sediment removal techniques are a high priority. On the other hand, dredging and excavating methods are not recommended on economic grounds, as they require special operational conditions and consume pump energy or mechanical equipment (Dreyer, 2018). Another method, which uses potential energy and does not employ external energy such as a pump, is

* Corresponding author.
*E-mail address:* Hadi.Haghjuie@Gmail.com (H. Haghjouei).

https://doi.org/10.1016/j.jher.2022.09.002
Received 17 August 2021; Received in revised form 18 May 2022; Accepted 20 September 2022
Available online 28 September 2022

**Nomenclature**

| | |
|---|---|
| *CBA* | Cost-benefit analysis |
| $D_{50}$ | Median size of sediment particles (m) |
| $D_c$ | depth of sediment flushing cone (m) |
| $D_{DBE}$ | Diameter of the DBE structure (m) |
| $D_o$ | Diameter of the bottom outlet (m) |
| $D_{SC}$ | Diameter of the PSC structure (m) |
| *DBE* | Dendritic bottomless extended |
| *E* | Flushing efficiency (dimensionless) |
| $Fr_o$ | Outlet flow Froude number (dimensionless) |
| $G_s$ | Specific gravity of the sediment (dimensionless) |
| $H_{bo}$ | Height of the low-level outlet from the reservoir bed (m) |
| $H_s$ | Sediment head above the orifice bottom (m) |
| $H_w$ | Total water head above the orifice (m) |
| $L_b$ | Length of flushing cone along the branch (m) |
| $L_c$ | Length of sediment flushing cone (m) |
| $L_d$ | Length of flushing cone at the concentration point of the outlet of branches (m) |
| $L_{DBE}$ | Length of the branches of the DBE structure (m) |
| $L_{SC}$ | Length of the branches of the PSC structure (m) |
| $L_x$ | Horizontal scale index (dimensionless) |
| $L_z$ | Vertical scale index (dimensionless) |
| *N* | Number of branches in the DBE structure (dimensionless) |
| $n_i$ | Inlet Manning surface roughness of DBE structure |
| $n_o$ | Outlet Manning surface roughness of DBE structure |
| *PSC* | Projecting semi-circular |
| $Q_o$ | Orifice outlet discharge ($m^3/s$) |
| *Re* | Reynolds number (dimensionless) |
| *SE* | The standard error lines represent the average distance the observed values fall from the regression line |
| $W_c$ | Width of sediment flushing cone (m) |
| $\theta$ | Angle between the branches of the DBE structure (degree) |
| $\theta_b$ | Angle of the removed circular sector of DBE structure (degree) |
| $\theta_f$ | Friction angle of the sediments (degree) |
| $\rho_s$ | Sediment density ($kg/m^3$) |
| $\rho_w$ | Fluid density ($kg/m^3$) |
| $\mu$ | Dynamic fluid viscosity (kg/ms) |
| $\forall_c$ | Volume of the sediment flushing cone ($m^3$) |
| $\forall_w$ | Volume of the evacuated water ($m^3$) |

the hydrosuction sediment-removal system (HSRS). HSRS has a lower operating cost than dredging and excavating and is usually applied in small reservoirs or where flushing is not possible (Kondolf et al., 2014).

Flushing has been used on various research sites for many years. Flushing is a hydraulic method of sediment removal through the bottom outlet of the dam, and is classified into two types, drawdown flushing (also known as free-surface or empty or free-flow flushing) and pressurized flushing (Morris and Fan, 2009). Sediment flushing can support the retrieval of storage lost due to siltation and sediment replenishment downstream through dams (Espa et al., 2019). Free-flow or drawdown flushing is carried out by creating riverine conditions and lowering the water level, and it is commonly practiced in small and medium reservoirs (Isaac and Eldho, 2019). Retrogressive erosion mainly occurs in drawdown flushing, creating a flushing channel upstream of the low-level outlet, but the flushing scour due to erosion is localized in pressure flushing (Fig. 1) (Meshkati et al., 2009).

The effectiveness of sediment flushing depends on hydraulic, hydrological, and topographical conditions and the operation of the bottom outlet (Isaac and Eldho, 2016; Trimble et al., 2012). To be effective, pressurized flushing is carried out with a moderate drawdown, whereas

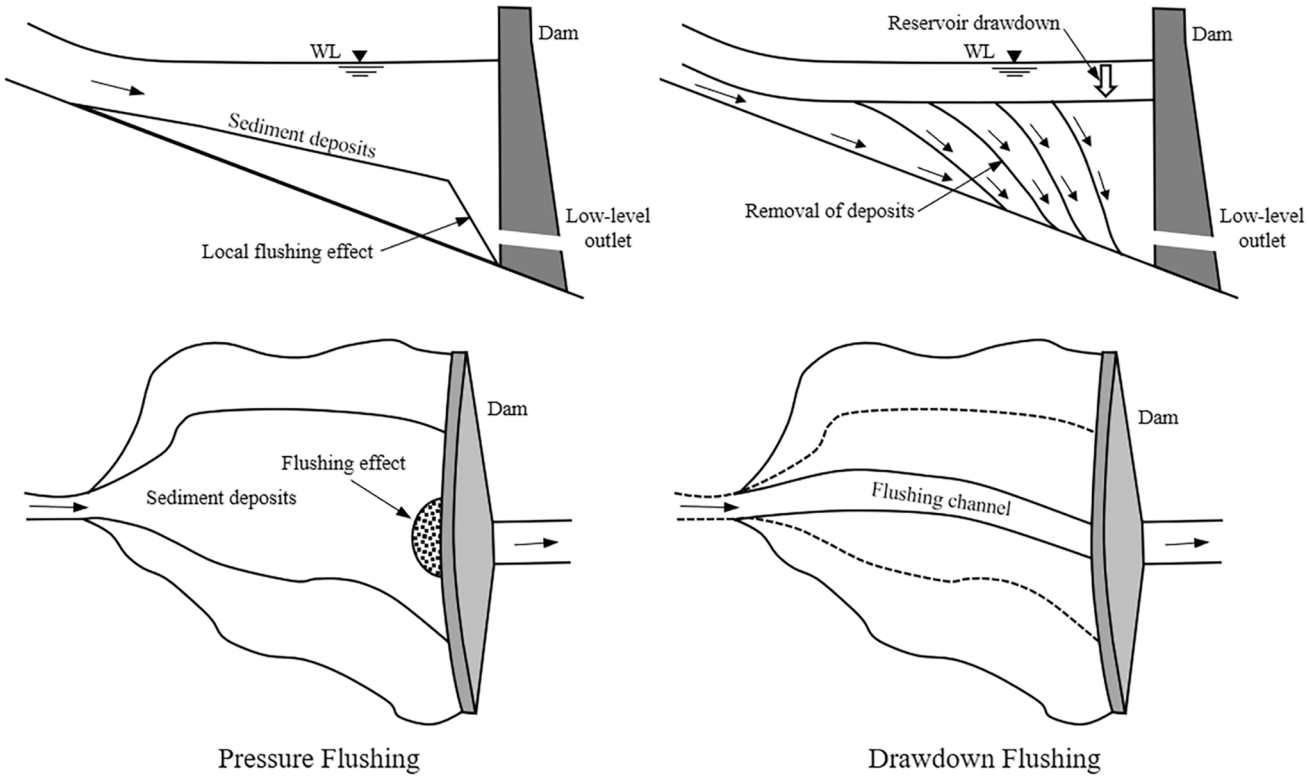


**Fig. 1.** Schematic representation of pressure flushing and drawdown flushing (Dreyer, 2018).

drawdown flushing requires a high drawdown and the water level reaches the height of the low-level outlet (Trimble et al., 2012). Drawdown flushing leads to increased sediment loads and low water quality, which can threaten life in downstream watercourses (e.g., fish mortality) (Baoligao et al., 2016; Malavoi and El Kadi Abderrezzak, 2019; Stähly et al., 2019). It should be noted that in some cases (e.g., periphyton mats and filamentous green algae), flushing in and of itself cannot modify the food web of the river and downstream of the dam (Katano et al., 2021). One of the main disadvantages of pressurized flushing is its low ability to recover a large storage capacity because of the localized effect near the bottom outlet. However, pressurized flushing keeps the power intake free of sediments, and the water loss is much less compared to drawdown flushing. Therefore, this method of flushing is more practical for hydropower dams in arid and semi-arid regions.

Many experimental and numerical studies have been conducted on pressurized flushing and the factors affecting increased efficiency and flushing volume. Most investigations have focused on the impacts of hydraulic factors (e.g., water height) on the bottom outlet, output discharge, the shape and diameter of the bottom outlet, the type and height of the sediments above the bottom outlet, and the temporal development of the flushing cone (Dreyer, 2018). For example, White and Bettess (1984) studied the interrelationship between the distance limits of scouring, reservoir depth, and outlet discharge. The results indicated that the scouring cone dimensions were increased by lowering the water level in the reservoir.

One-, two-, and three-dimensional numerical models are commonly applied to simulate the sediment flushing and reservoir sedimentation. One-dimensional models are used to investigate reservoir sedimentation, while two- and three-dimensional models investigate sediment flushing from reservoirs (Isaac and Eldho, 2019). The ensuing investigations have been reported: simulation of reservoir sedimentation and flushing of the Xiaolangdi reservoir with 1D GSTARS3 (Ahn and Yang, 2010; Ahn, 2011); evaluation of reservoir flushing of the Kali Gandaki hydropower reservoir in Nepal with a 3D numerical model of SSIIM (Haun and Olsen, 2012); simulation of sediment flushing of the Pieve di Cadore reservoir with a system of numerical models (Gallerano et al., 2016); simulation of flood events and consequent river scouring and deposition behaviors Jhong-Jhuang Bank-Side Reservoir with CCHE1D (Chao et al., 2021); evaluation of the effect of the supplied sediment on the spawning redds of Ayu fish in the Tenryu River with CCHE2D (Kantoush et al., 2018); estimation of the reservoir sedimentation profile of the Punatsangchhu with HEC-RAS 4.1 (Isaac and Eldho, 2019); and prediction of the local sediment flushing scour upstream of the bottom outlet with a coupled fully 3D numerical model (Sawadogo et al., 2019).

Experimental investigations have been carried out on laboratory models to study various aspects of sediment flushing phenomena (Isaac and Eldho, 2019). Using a physical model of a reservoir, Talebbeydokhti and Naghshineh (2004) concluded that the volume of the flushing cone was a function of outlet discharge, water height, and the width of the flushing channel. Emamgholizadeh et al. (2006) experimentally investigated factors influencing the volume of the flushing cone and concluded that this parameter was a function of flow characteristics and the type of sediments. Powell and Khan (2015) investigated the effect of flow characteristics on the formation of the flushing cone. They reported that the vortices formation near the bottom outlet and the local impact of the bottom outlet were the essential factors in the mechanism of pressurized flushing. Meshkati et al. (2009) studied the temporal changes of flushing cone development. They concluded that the scour depth was greater in the more significant outflow at a constant water height of the reservoir and in a specific time. All the above studies similarly explored the usual conditions affecting a reservoir, whereas less attention has been paid to structural effects influencing the formation of vortices, turbulence, and an increase in sediment removal. Ahadpour Dodaran et al. (2012) studied the impact of localized vibrations on the dimensions of the flushing cone. They found that the highest diameter of outlet and vibration frequency led to creating the largest flushing cone.

Furthermore, the cross-section area of the output current and the vibration frequency was also essential parameters affecting the dimensions of the flushing cone. Althaus et al. (2014) investigated the effects of geometrical parameters and jet discharge and concluded that the flushing efficiency depended on the experiment duration and flow pattern. Madadi et al. (2016) studied the effect of a circular pile group structure on flushing efficiency, obtaining the best results when the diameter of the piles and their distances from one another were the same. They also found that using the pile group in flushing increased the flushed volume by up to 250 % compared to the reference test (without a structure). Madadi et al. (2017) investigated the effect of a projecting semi-circular structure (PSC) on flushing efficiency. This structure was connected to the dam's bottom outlet and pillars on another side. The authors found that the most significant amount of sediment flushing occurred when the PSC diameter dimensionless index ($D_{sc}/D_o$) was equal to 1.32 and the PSC length dimensionless index ($L_{sc}/D_o$) was equal to 5.26; in this case, the volume of the flushing cone was 4.5 times more than the reference test. Beiramipour et al. (2021) studied the effect of submerged vane characteristics (heights, angles, spacing, and arrangements) on sediment flushing efficiency. The results indicated that in the presence of submerged vanes, final sediment flushing efficiency increased by a factor of 48 compared to the reference test. Finally, Haghjouei et al. (2021) experimentally investigated the effect of a dendritic bottomless extended (DBE) structure at three angles of 30°, 45°, and 60° between the branches, three sediment levels for three discharge rates. The results indicated that the highest sediment level and discharge rate in the Angle of 30° led to the maximized sediment removal efficiency (10-fold in compression with the reference test).

As mentioned above, one of the main disadvantages of pressurized flushing is its low ability to recover a large amount of storage capacity because of a localized effect near the bottom outlet. In Haghjouei et al.'s (2021) study, the impact of the Angle between the branches of the DBE structure has been investigated, and the other physical parameters of the structure consist of the length and the diameter of the structure was constant. Therefore, this research examines the effects of the length and the diameter of DBE on sediment removal efficiency under pressurized flushing.

## 2. Methods and materials

### 2.1. Methodology

This study investigates the effects of using a dendritic, bottomless, extended structure of various lengths and diameters for multiple discharges on the pressurized sediment flushing of reservoirs. For this purpose, a physical and hydraulic model of the dam and water conduit was designed and constructed in the Hydraulic and Water Structures Research Laboratory in Shahid Bahonar University, Kerman, Iran.

Experiments were carried out with three different discharges, four diameters, and four different structure lengths to design dimensions of the structure that removed sediment most efficiently. The results were compared with the reference test in the same laboratory conditions. The results revealed the best dimensions of the structure, and accordingly, the equations describing the sediment cone geometry were developed based on regression analysis.

### 2.2. Description of the physical model

The present model comprises a rectangular prism with 7.5 * 3.5 * 1.8 (m) dimensions in length, width, and height, respectively. The model consists of the main reservoir, water conduit, sediment-trapping box, flow dissipater areas at inlet and outlet flow, and flow measurement facilities (volumetric flow meter for inlet flow and V-notch weir for outlet flow). The schematic view (Fig. 2) shows that, at a distance of 50

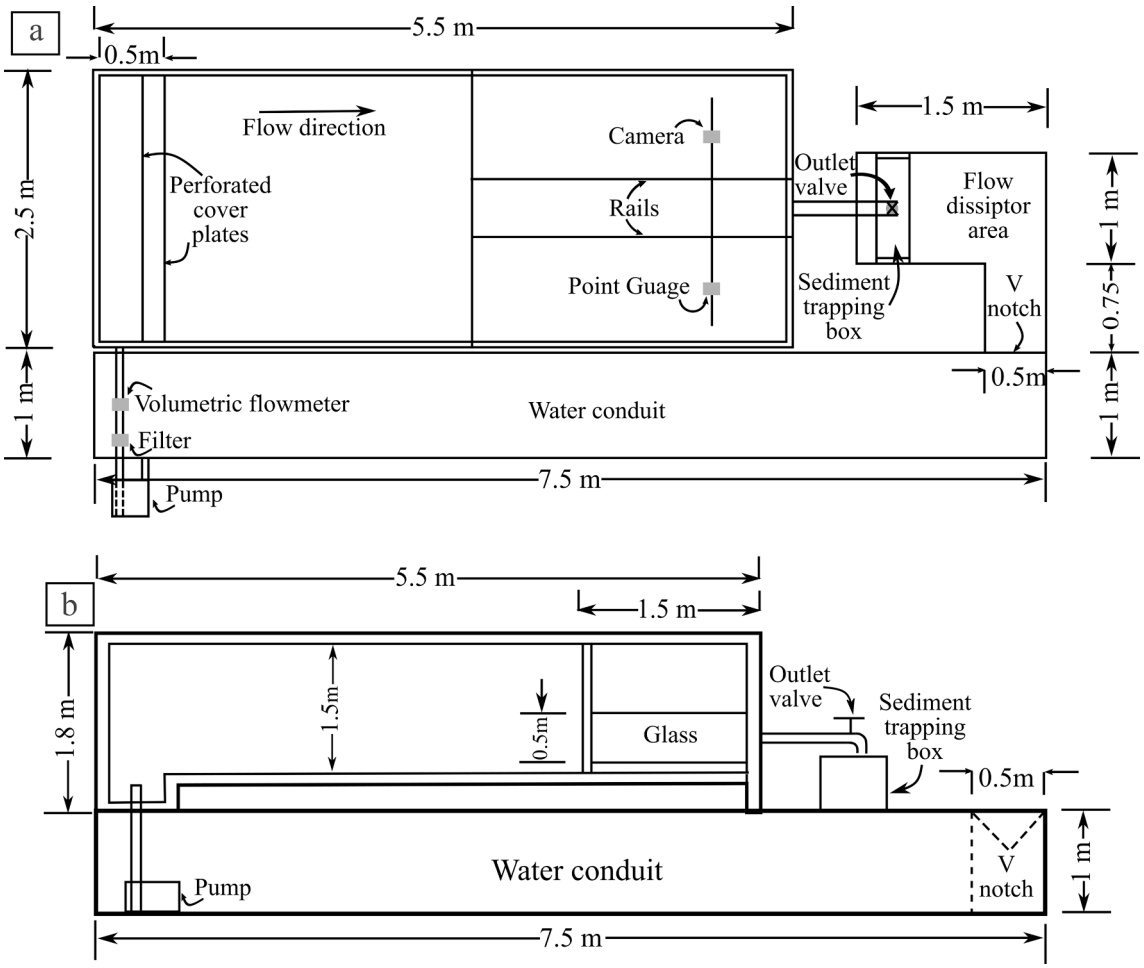


**Fig. 2.** Schematic representation of the physical model, plan (a), and side view (b).

cm from the beginning of the reservoir, there are two perforated cover plates for reducing the turbulence of the inlet flow to the reservoir. It should be noted that the reservoir model is 5.5 m long, 2.5 m wide, and 1.8 m high. The inlet and outlet flows are measured by a volumetric flow meter and a triangular weir with a 90-degree, respectively. The current physical model was a distorted physical model that matched existing dams. For instance it matched Jiroft Dam in Kerman, Iran, with the horizontal and vertical scale indices of $L_x = 1/110$ and $L_z = 1/90$, respectively. According to the mentioned scales, the discharge of 20 L/s in model was equivalent to outlet discharge of 1900 $m^3/s$ in the Jiroft Dam, as the prototype.

Non-cohesive silica sediment with a median diameter of $D_{50} = 0.73mm$ and a relative density of 2.625 was used in this study (Haghjouei et al., 2021).

### 2.3. DBE structure

Despite the high importance of increasing sediment removal efficiency, most previous studies have concentrated on ascertaining the flushing mechanism and the effect of hydraulic parameters on the dimensions of the sediment flushing cone. Madadi et al. (2017) utilized a new configuration of the dam bottom outlet, a PSC structure, to increase the efficacy of sediment evacuation. PSC can flush at a direct path leading to the bottom outlet. Haghjouei et al. (2021) proposed a new structure configuration involving a dendritic, bottomless, extended structure (DBE structure) with the ability of flushing at different sides of the reservoir in addition to the direct path. The DBE structure consists of several branches with an angle of $\theta$ between them. The authors focused on the effects of the variation of $\theta$, sediment level, and discharge rate on sediment removal efficiency. In the current research, other structural characteristics consisting of the diameter and length of the structure have been investigated. Also, one of the main DBE structure characteristics was the Angle of the removed circular sector that depends on the DBE diameter ($\theta_b$) (Fig. 3). Here, considering that the effect of $\theta$ had been already investigated in the recent study, it reminded constantly according to the best operation of $\theta$ in the previous study ($\theta = 30^{\circ}$). Also, the Number of the branches of the DBE structure ($N$) remained constant ($N = 3$). The DBE structure characteristics in Haghjouei et al. (2021) and the current study have been compared in Table 1. The probability of instability of the structure was negligible, thanks to its circular cross-section. As in the PSC structure, because of this circular shape, the concentration stresses on the structure's crown and the vertical forces are transferred to the reservoir bed through piles (Madadi et al., 2017). The presence of structural branches in different aspects of the reservoir is an excellent advantage of the DBE structure, leading to an increase in the sediment removal domain and limiting the distances of scour from the outlet (Haghjouei et al., 2021). The structures were linked to the bottom outlet from one side and through the metal bases to the deposited sediment (Fig. 4).

### 2.4. Test program

Before starting and doing each test, the outlet discharge situation in the physical model was investigated. The primary results indicated that discharge rates less than 12 L/s are not appropriate for pressure flushing and more than 18 L/s are not controllable to create balance and constant

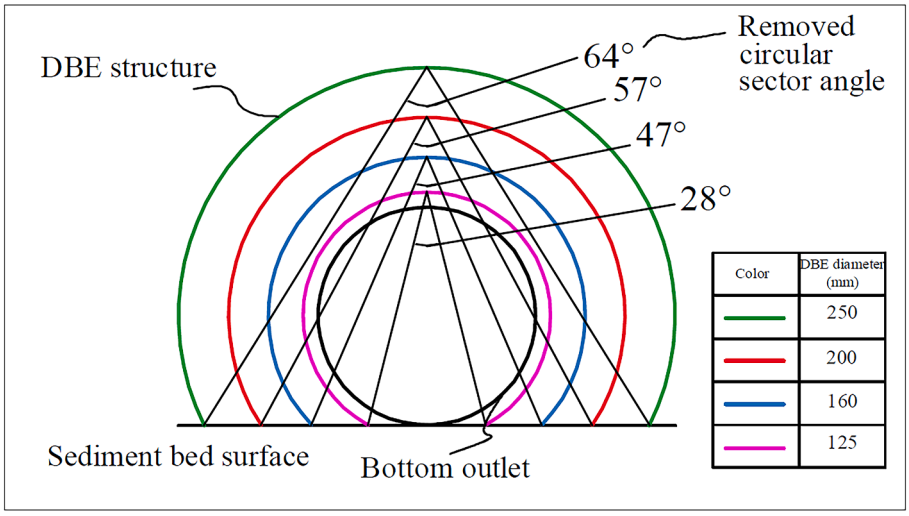


**Fig. 3.** Schematic representation of the Angle of DBE removed circular sector, front view.

**Table 1**
DBE structure characteristics in Haghjouei et al. (2021) study vs the current study.

| DBE structure characteristics | | |
|---|---|---|
| Type of DBE characteristics | Haghjouei et al. (2021) | The current study |
| Length (m) | 0.8 | 0.3, 0.5, 0.8, 1.1 |
| Diameter (m) | 0.16 | 0.125, 0.16, 0.2, 0.25 |
| Angle between the branches (degree) | 30, 45, 60 | 30 |
| The Number of the branches | 3 | 3 |

height in the model. Consequently, the experiments were carried out for three discharges of 12.5, 15, and 18 L/s. Also, the four different diameters and four different lengths of the DBE structure, were investigated. The experiments were done for a constant sediment level in no-blockage mode with a height of 39.5 cm from the reservoir bed. The water level for all the tests was constant and equal to 65 cm. The experimental data for 48 experiments are shown in Table 2.

### 2.5. Test procedure

Each test was done by turning on a low-rate foam pump to prevent the degradation of the sediment surface at the beginning. A centrifugal pump turned on and the low-level outlet valve opened after the reservoir water level reached to the desired level that controlled by a manual pointer gauge with a precision of ±1 mm and rulers were mounted on the sides of the reservoir (Haghjouei et al., 2021). The inlet flow and the outlet flow were checked every 20 min. The equilibrium condition was reached at 270 min. But all the experiments continued for 120 min. It should be noted that the variation of flushing cone dimensions between 120 and 270 min was less than 1 mm. Consequently, the time duration of each test was considered 120 min. After the end of each experiment, the completion of each test, and ensuring complete drainage of the main reservoir, 3D sedimentary bed models using close-range photogrammetry through a photo scanning technique (PST) of photo images captured using an advanced Canon IXUS 190 with remote control facility, have been made and was used to obtain the topography of the sediment flushing cone. The model accuracy was calculated in reference to checkpoints, and the results illustrated that the minimum accuracy was 0.512 % and 0.58 % for the range of <1 m and 1–2 m, respectively. Also, the typical accuracy (RMSE) was 0.26 % and 0.31 % for the field of <1 m and 1–2 m, respectively.

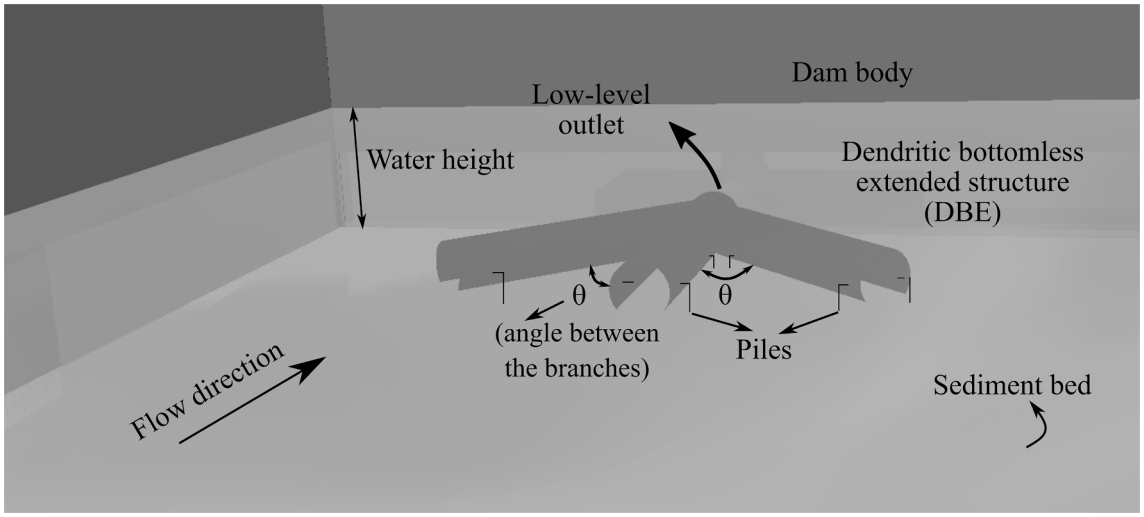


**Fig. 4.** Schematic representation of the DBE structure connected to upstream of the dam body (Haghjouei et al., 2021).

**Table 2**
Experiments carried out in the present research.

| Test No. | $D_{DBE}$ (cm) | $L_{DBE}$ (cm) | $Q_o$ (L/s) | Test No. | $D_{DBE}$ (cm) | $L_{DBE}$ (cm) | $Q_o$ (L/s) | Test No. | $D_{DBE}$ (cm) | $L_{DBE}$ (cm) | $Q_o$ (L/s) |
|---|---|---|---|---|---|---|---|---|---|---|---|
| 1 | 125 | 30 | 12.5 | 17 | 125 | 30 | 15 | 33 | 125 | 30 | 18 |
| 2 | 160 | | | 18 | 160 | | | 34 | 160 | | |
| 3 | 200 | | | 19 | 200 | | | 35 | 200 | | |
| 4 | 250 | | | 20 | 250 | | | 36 | 250 | | |
| 5 | 125 | 50 | | 21 | 125 | 50 | | 37 | 125 | 50 | |
| 6 | 160 | | | 22 | 160 | | | 38 | 160 | | |
| 7 | 200 | | | 23 | 200 | | | 39 | 200 | | |
| 8 | 250 | | | 24 | 250 | | | 40 | 250 | | |
| 9 | 125 | 80 | | 25 | 125 | 80 | | 41 | 125 | 80 | |
| 10 | 160 | | | 26 | 160 | | | 42 | 160 | | |
| 11 | 200 | | | 27 | 200 | | | 43 | 200 | | |
| 12 | 250 | | | 28 | 250 | | | 44 | 250 | | |
| 13 | 125 | 110 | | 29 | 125 | 110 | | 45 | 125 | 110 | |
| 14 | 160 | | | 30 | 160 | | | 46 | 160 | | |
| 15 | 200 | | | 31 | 200 | | | 47 | 200 | | |
| 16 | 250 | | | 32 | 250 | | | 48 | 250 | | |

### 2.6. Dimensional analysis

The sediment flushing cone volume ($\forall_c$) depends on several variables: fluid viscosity ($\mu$), outflow discharge ($Q_o$), total water head above the orifice ($H_w$), sediment head above the orifice bottom ($H_s$), the height of the low-level outlet from the reservoir bed ($H_{bo}$), the median size of sediment ($D_{50}$), sediment density ($\rho_s$), fluid density ($\rho_w$), acceleration due to gravity ($g$), the diameter of the low-level outlet ($D_o$), the diameter of the DBE structure ($D_{DBE}$), length of the branches of the DBE structure ($L_{DBE}$), Angle between the branches of the DBE structure ($\theta$), Angle of the removed circular sector of DBE structure ($\theta_b$), inlet surface roughness of DBE structure ($n_i$), outlet surface roughness of DBE structure ($n_o$), friction angle of sediments ($\theta_f$), and the number of branches ($N$), as follows:

$$\forall_c = f(Q_o,\ H_w, H_s, H_{bo}, D_{50},\ \rho_w,\ \rho_s,\ \mu,\ g,\ D_o,\ D_{DBE},\ L_{DBE}, n_i,\ n_o,\ \theta, \theta_b, \theta_f, N) \quad (1)$$

Using Buckingham $\pi-$ theorem, the resulting terms of the dimensional analysis are obtained as:

$$\frac{\forall_c}{D_o{}^3} = f_1\left(\frac{H_w}{D_o}, \frac{H_s}{D_o}, \frac{H_{bo}}{D_o}, \frac{D_{50}}{D_o}, \frac{D_{DBE}}{D_o}, \frac{L_{DBE}}{D_o}, n_i, n_o, \theta, \theta_b, \theta_f, \frac{\rho_s}{\rho_w}, \frac{4\rho Q_o}{\mu\pi D_o}, \frac{Q_o}{\frac{\pi}{4}\sqrt{g{D_o}^5}}, N\right) \quad (2)$$

By multiplying $\frac{H_s}{D_o}$ and inverse of $\frac{H_{bo}}{D_o}$, a new parameter of $\frac{H_s}{H_{bo}}$ can be obtained that indicated the rate of obstruction. Also, according to the relations of $G_s = \frac{\rho_s}{\rho_w}$, $Fr_o = \frac{Q_o}{\frac{\pi}{4}\sqrt{g{D_o}^5}}$, and $Re = \frac{4\rho Q_o}{\mu\pi D_o}$, the Eq. (2) is obtained as:

$$\frac{\forall_c}{D_o{}^3} = f_2\left(\frac{H_w}{D_o}, \frac{H_s}{H_{bo}}, \frac{D_{50}}{D_o}, \frac{D_{DBE}}{D_o}, \frac{L_{DBE}}{D_o}, n_i, n_o, \theta, \theta_b, \theta_f, G_s, Re, Fr_o, N\right) \quad (3)$$

In all the tests, the sediment specific gravity ($G_s$) was constant. The friction angle of the sediment ($\theta_f$) depends on the grain size and shape and remained constant in all the tests. Also, the Angle of the removed circular sector of the DBE structure ($\theta_b$), depends on the DBE diameter. Therefore, it was considered negligible in the current research to maintain the independent variables. Inlet and outlet Manning surface roughness of DBE structure ($n_i$ and $n_o$, respectively), reminded constantly in all the tests, Due to using the same structural material in this study. The Reynolds number ($\frac{4\rho Q_o}{\mu\pi D_o}$) was considered negligible under a fully turbulent flow from the orifice. In addition, $D_{50}$, $H_s$, $H_w$ , $\theta$, and $N$ were constant and, therefore, $\frac{D_{50}}{D_o}$, $\frac{H_s}{H_{bo}}$ , $\frac{H_w}{D_o}$, $\theta$, and $N$ remained constant in this experimental study. The constant dimensionless values are shown in Table 3.

Eq. (3) can be simplified as follows:

$$\frac{\forall_c}{D_o{}^3} = f_3\left(\frac{L_{DBE}}{D_o}, \frac{D_{DBE}}{D_o}, Fr_o\right) \quad (4)$$

**Table 3**
Constant dimensionless values.

| $\frac{D_{50}}{D_o}$ | $\frac{H_s}{H_{bo}}$ | $\frac{H_w}{D_o}$ | $N$ | $\theta$ | $G_s$ | $\theta_f$ | $n_i$ | $n_o$ |
|---|---|---|---|---|---|---|---|---|
| 0.00664 | 1 | 5.909 | 3 | 30° | 2.625 | 29° | 0.011 | 0.011 |

Where $D_o = 0.11\,m$ and.$H_{bo} = = 0.395\,m$

According to Eq. (4), the dimensionless variation of $L_{DBE}$, $D_{DBE}$, and $Fr_o$ will be investigated here to determine the optimal dimensions. In fact, the sediment flushing cone volume will be changed with the variation of sediment flushing cone length, width, and depth ($L_c$, $W_c$, and $D_c$, respectively) and several variables can affect the sediment flushing cone dimensions.

## 3. Results and discussion

As shown in Table 2, DBE structures with different lengths and diameters were used to design the experiments. The results were compared with the reference test, i.e., without the structure mode.

The first phase of the experiment discharges a volume of sediments by opening the bottom outlet and creating turbulence on the two sides of the bottom outlet. This phase takes less than 1 min, consistent with recent studies, e.g., Madadi et al. (2017) and Haghjouei et al. (2021). The next phase is the simultaneous creation of vortices and outlet flow. These vortices lead to the discharge of sediments by intermittent performance under and on the two sides of the bottom outlet and movement from the branches and reaching a concentrated point near the bottom outlet results in the creation of a strong vortex, called the central vortex, especially under the bottom outlet (Haghjouei et al., 2021). The next type of vortices is created from piping erosion in length and two sides of the structure, owing to a pressure difference inside and outside the system along the branches (Madadi et al., 2017). The common point of all the experiments was that 90 % of the flushing operation was conducted within an interval of 15–20 min, and variation of flushing cone dimensions between 120 and 270 min was less than 1 mm (Fig. 5).

### 3.1. Investigation of the changes in the sediment flushing cone geometry caused by increases in the length and diameter of the structure

After conducting each experiment, the length, width, and depth of the flushing cone were measured in addition to taking photos of different points. Accordingly, three graphs were constructed related to variations in the flushing cone's length, width, and depth for other modes of the structure diameter and length variations (Fig. 6). Examination of

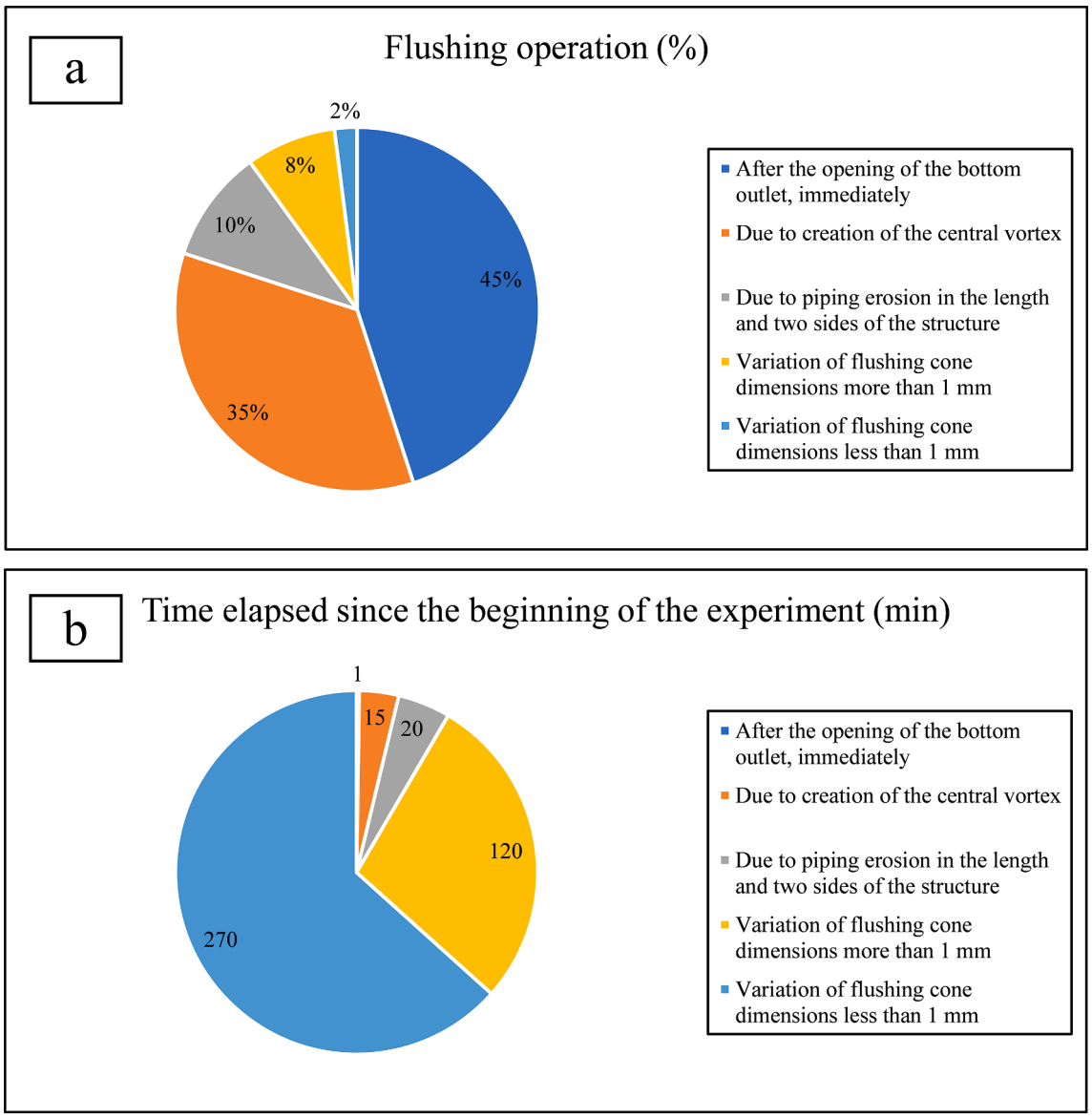


**Fig. 5.** Sediment flushing phases observed in the present research, flushing operation (a), and time elapsed since the beginning of the experiment (b).

sediments indicated that, as the dimensionless index of the structure length of $L_{DBE}/D_o$ increased from 2.73 to 10, the length of the flushing cone increased by a maximum of 6.6 times more than the reference test and 2.4 times more than $\frac{L_{DBE}}{D_o} = 2.73$. By increasing this length, the width of the flushing cone increased by a maximum of 1.75-fold, and the depth of the sediment cone increased by a maximum of 1.33-fold compared with the reference test.

Although the changes in length indicate the difference between the width and depth of the flushing cone when not in structure mode, the notable point is that, in the same discharge, there were no significant changes in the flushing cone width and depth in different methods of increase of the length of the structure, showing a constant trend.

For comparison, the longitudinal profile of the flushing cone was first drawn to study the effect of a length increase. By examining the flushing cone created by the structure, it can be concluded that the flushing cone influenced by the DBE structure is divided into two parts (Fig. 7): A) flushing cone at the concentration point of the outlet of branches (Ld), resulting from first progressive erosion and then retrogressive erosion; in fact, the latter occurs due to hydraulic energy changes caused by the discontinuous longitudinal profile; B) flushing cone along the branch (Lb), resulting from piping erosion, which occurs due to the pressure difference between the inside and outside of each branch.

A much broader and deeper flushing cone resulting from stronger vortices was produced by the presence of the concentration point of the outlet from branches. The cone also has an average flushing volume of 55 % since the maximum speed of the outflow, which is the leading cause of the turbulence, is concentrated near the outlet. The effect of speed is less on the other points lying farther distant from the outlet point. Because of the pressure difference between the two sides of the branches, however, another type of flushing cone is created along the branches longitudinally, with less width and depth than that near the bottom outlet and having an average flushing volume of 45 %. In this respect, the length of the flushing cone can be understood as the direct length and the length of the branches. However, it should be mentioned that, in the current research, $L_d$ is considered constant and $L_b$ includes increasing the distance. Determining the optimal dimensions of $L_d$ and $L_b$ and changes at the length of the direct branch relative to side branches can be investigated in further studies.

In order to investigate more precisely the effect of an increase in the structure length, the flushing cone longitudinal profile, according to the coordinates system of the experimental setup shown in Fig. 8, was drawn in size dimensionless ratios of 2.73–10 (Fig. 9). The results show that the

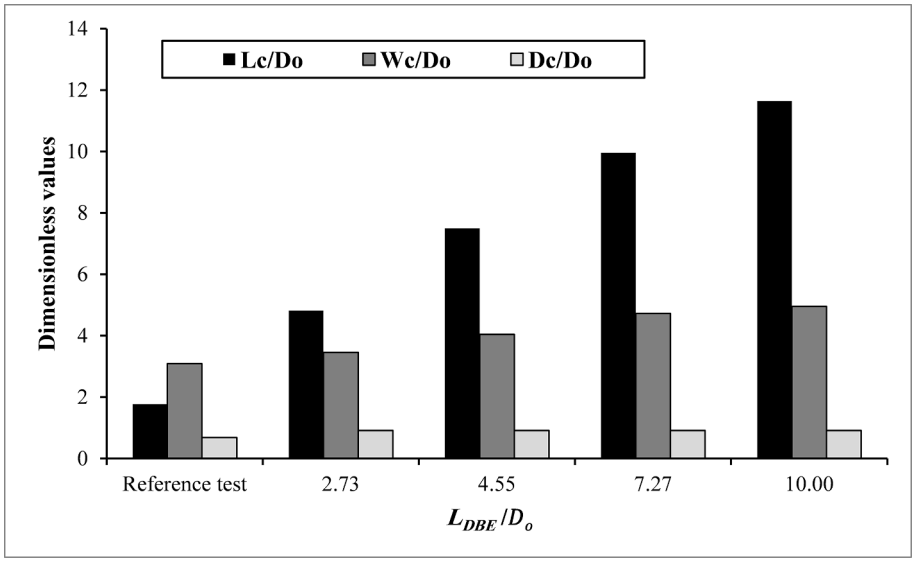


**Fig. 6.** Variations of the flushing cone at different $L_{DBE}/D_o$ values.

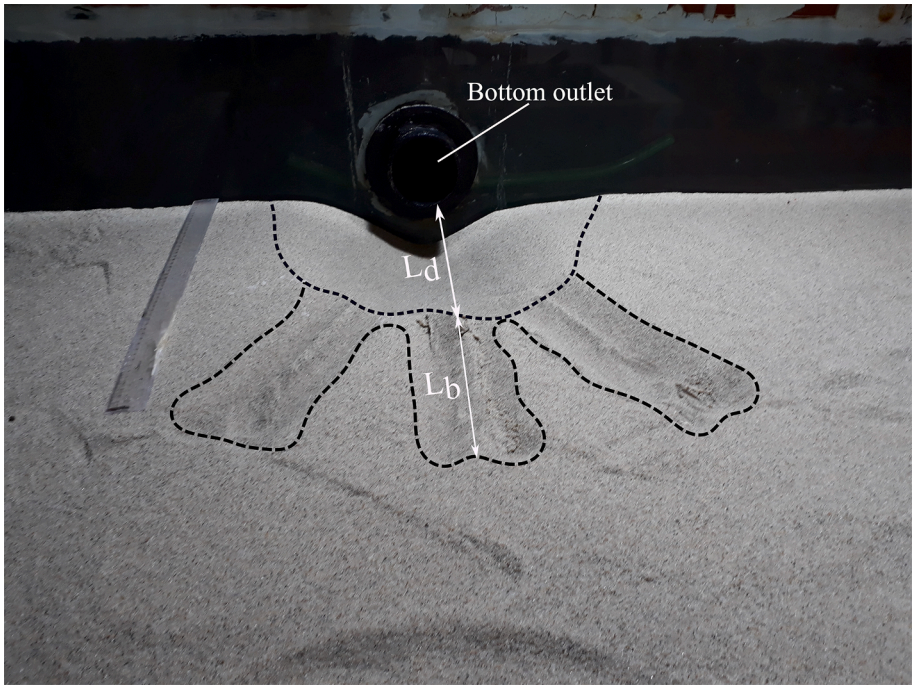


**Fig. 7.** Representation of flushing cone parts.

turbulence and the local impact on the sediments have moved away from the bottom outlet to other parts of the reservoir, owing to a pressure difference between the inside and the outside of each branch, creating piping erosion. This indicates that, in pressure flushing, by installing the structure upstream of the bottom outlet, not only does the local impact of the bottom outlet lead to flushing but also the pressure difference between the two sides of the structure along the branches causes erosion, sediment suspension, and their movement to the bottom outlet. This means that, of the dimensionless indices of length, the structure with $\frac{L_{DBE}}{D_o} = 10$ has the best function.

The sediment flushing cone cross-sectional data can be used to investigate the structure's operation and compare it with the reference test. To achieve more precision, the changes to the bottom outlet in the transverse cross-sections of the flushing cone profile at two dimensionless values of $Y/D_o = 0.5$ and $Y/D_o = 1$ were investigated in test nos. 33, 37, 41, and 45. In this regard, the positive directions of the X, Y, and Z axes were considered according to the coordinates system of the experimental setup (Fig. 8). Accordingly, changes in the profile based on the third dimension are extracted as Fig. 10.

It is clear from comparison with the reference test that the best profile for the DBE structure profiles is that with the closest distance to the outlet ($Y/D_o = 0.5$). The results indicate that the depth of the flushing cone for different modes of structure diameters decreased owing to the distance from the concentrated point (central vortices) near the bottom outlet. Also, the inter-comparison between different modes of length dimensionless index of the DBE structure show that the structure with $\frac{L_{DBE}}{D_o} = 10$ has the maximum transverse cross-sectional area.

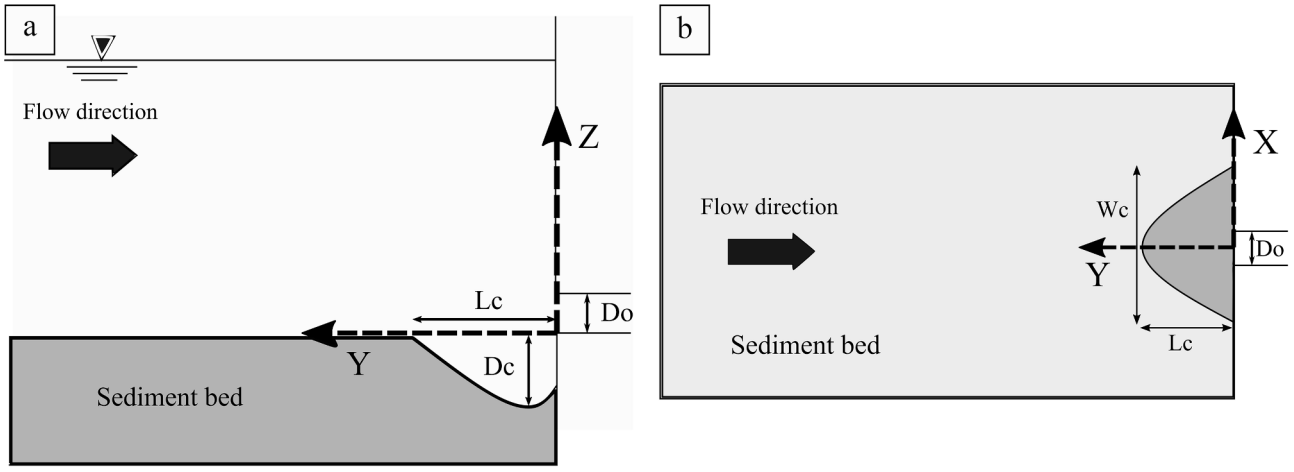


**Fig. 8.** Coordinates system of experimental setup, side view and plan (a and b, respectively).

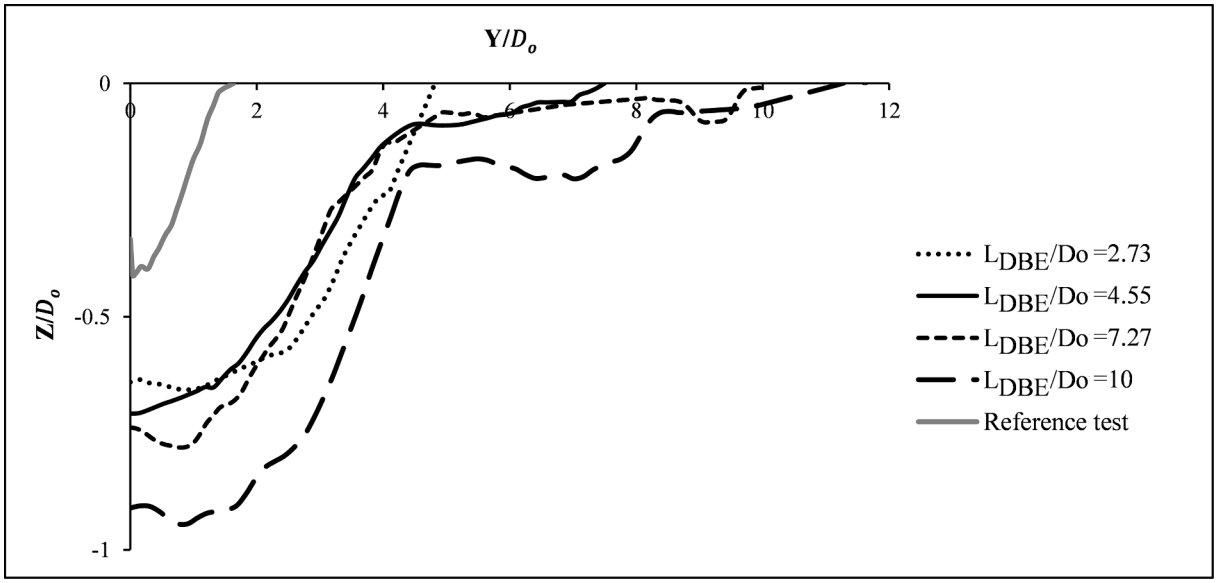


**Fig. 9.** Flushing cone longitudinal profile at different $L_{DBE}/D_o$ values.

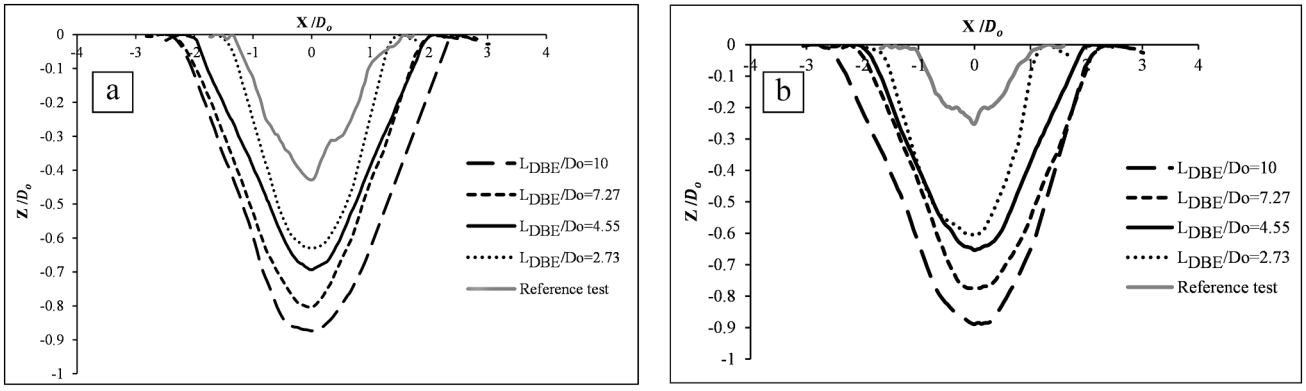


**Fig. 10.** Transverse cross-section of flushing cone in test nos. 33, 37, 41, and 45 for $Y/D_o = 0.5$ (a) and $Y/D_o = 1$ (b).

On increasing the structure diameter, the effect of changes in the diameter dimensionless index of $D_{DBE}/D_o$ were compared with the reference test, i.e., the structure-less mode. It was found that the length, width, and depth of the flushing cone showed an increase in $D_{DBE}/D_o$ values from 1.14 to 2.27, but the maximum length of the flushing cone was $\frac{D_{DBE}}{D_o} = 1.14$. More speed and increases in the shear stress and the resulting force arise from the lower cross-sectional area of the flow at

smaller diameters. A higher rate leads to the excavation and suspension of sediment particles, increasing sediment removal. This also counters the claims by Morris (2015) about the insignificant effect of speed on sediment removal in pressure flushing. In the present study, $\frac{D_{DBE}}{D_o} = 1.14$ was obtained as an optimized diameter dimensionless index. Moreover, in the same discharge, changes in the width and length of the flushing cone in different types of increase in $D_{DBE}$ were not considerably different from one another and demonstrated a relatively steady trend (Fig. 11).

To investigate more precisely the effect of an increase in $D_{DBE}$, the flushing cone longitudinal profile was drawn from 1.14 to 2.27 in $D_{DBE}/D_o$ (Fig. 12). The results show that, among the dimensionless indices of diameter, the structure with the dimensionless index of $\frac{D_{DBE}}{D_o} = 1.14$ had the best operation.

Also, according to the transverse cross-section profiles of the sediment flushing cone in test nos. 45, 46, 47, and 48 for two different distances of $Y/D_o = 1$ and $Y/D_o = 6.36$ from the outlet, as presented in the coordinates system, the structure with $\frac{D_{DBE}}{D_o} = 1.14$ had the maximum transverse cross-sectional area (Fig. 13).

The results show that the DBE structure with the diameter dimensionless index of $\frac{D_{DBE}}{D_o} = 1.14$ was able to create a deeper and broader flushing cone than a greater diameter dimensionless index because of the enclosure of the flow and an increase in the shear stress. Also, the latter had a decreasing trend, moving along the Y-axis and receding from the center of the bottom outlet.

The interrelationships between the distance limits of scour from the outlet and outlet discharge are shown in Fig. 14-a for different structure diameters and Fig. 14-b for different structure lengths. It can be seen that the distances of scour from the outlet increase as the structure's length increases, the structure's diameter decreases, and the outlet discharge increases. Thus, the best operation of the DBE structure is attained for a structure with dimensionless indices of $\frac{L_{DBE}}{D_o} = 10$ and $\frac{D_{DBE}}{D_o} = 1.14$ (test no.45).

Another case considered in this paper is the effect of increasing the outlet flow Froude number ($Fr_o$) on the dimensions of the flushing cone. Our findings indicate that an increase in this index from 1.26 to 1.82 leads to increases of 1.13 times and 1.23 times in the length and width of the flushing cone, respectively, with an almost constant depth of the cone (Fig. 15).

Based on the experimental results, Eqs. (5)–(7) represent the relationship between the sediment flushing cone dimensionless index and the main variables in Eq. (4), consisting of the DBE length dimensionless index for $2.73 \le \frac{L_{DBE}}{D_o} \le 10$, the DBE diameter dimensionless index for $1.14 \le \frac{D_{DBE}}{D_o} \le 2.27$, and the outflow discharge dimensionless index for $1.26 \le Fr_o \le 1.82$.

$$\frac{L_c}{D_o} = 2.307\left(\frac{L_{DBE}}{D_o}\right)^{0.672}\left(\frac{D_{DBE}}{D_o}\right)^{-0.231}(Fr_o)^{0.399} \quad R^2 = 0.981 \tag{5}$$

$$\frac{W_c}{D_o} = 2.801\left(\frac{L_{DBE}}{D_o}\right)^{0.068}\left(\frac{D_{DBE}}{D_o}\right)^{-0.201}(Fr_o)^{0.588} \quad R^2 = 0.907 \tag{6}$$

$$\frac{D_c}{D_o} = 0.641\left(\frac{L_{DBE}}{D_o}\right)^{0.97}\left(\frac{D_{DBE}}{D_o}\right)^{-0.139}(Fr_o)^{0.244} \quad R^2 = 0.891 \tag{7}$$

### 3.2. Temporal development of the sediment flushing cone

The tests were continued until the variation in the dimensions of the sediment flushing cone was negligible. The sediment cone starts to develop immediately after opening the low-level outlet valve when a high turbulent flow is created. In the present study, this process decreased with time, and approximately 90 % of the scouring process occurred in the first 15–20 min after the start of each experiment. The time duration of scouring equilibrium was 270 min. Still, at about 120 min after the start of each experiment, the variation in the scouring process decreased, and approximately 98 % of the variation rate of sediment flushing occurred. The comparison of the temporal development of the sediment flushing cone in the reference test with the best operation of the DBE structure (dimensionless indices of $\frac{L_{DBE}}{D_o} = 10$ and $\frac{D_{DBE}}{D_o} = 1.14$, test no. 45) is shown in Fig. 16. The observations revealed that, by connecting the DBE structure upstream of the low-level outlet, the rate of the temporal development of the sediment flushing cone increased significantly compared with the reference test.

### 3.3. Investigation of the volume of the sediment flushing cone

In this research, the volume of the sediment flushing cone was calculated according to the difference between the surfaces before and after the tests. The largest volume was found in test no. 45 with the dimensionless indices of $L_{DBE}/D_o = 10, D_{DBE}/D_o = 1.14$, and $Fr_o = 1.82$, equal to 0.030475 cubic meters, showing an increase of 36.55 times that of the reference test. The comparison of the sediment flushing cone volume in the reference test with the best operation of the DBE structure is shown in Fig. 17 using Surfer 21.

Based on the experimental results, Eq. (8) represents the relationship

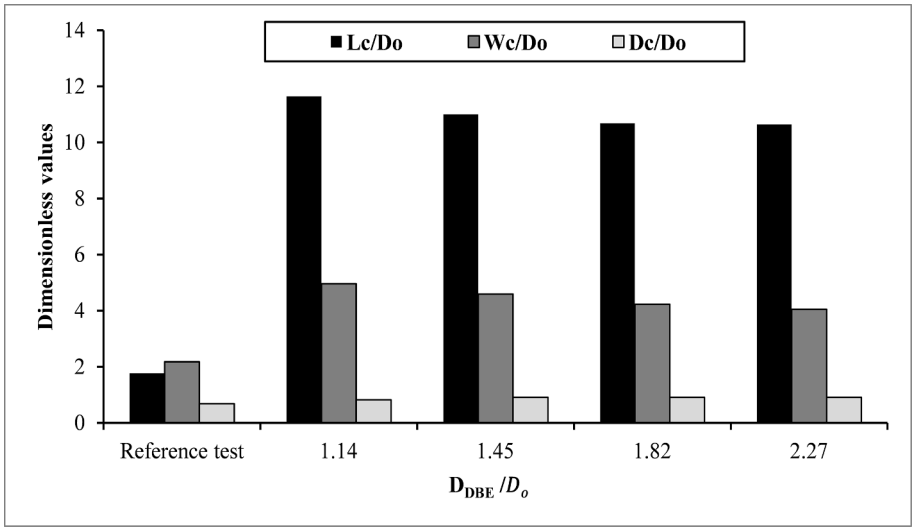


**Fig. 11.** Variation of flushing cone at different $D_{DBE}/D_o$ values.

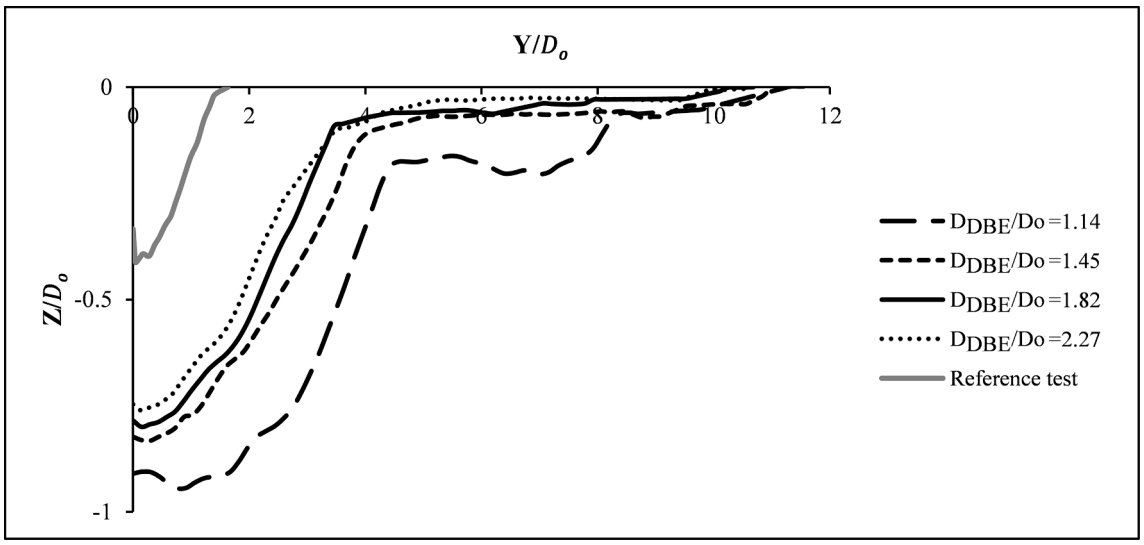


**Fig. 12.** Flushing cone longitudinal profile at different $D_{DBE}/D_o$ values.

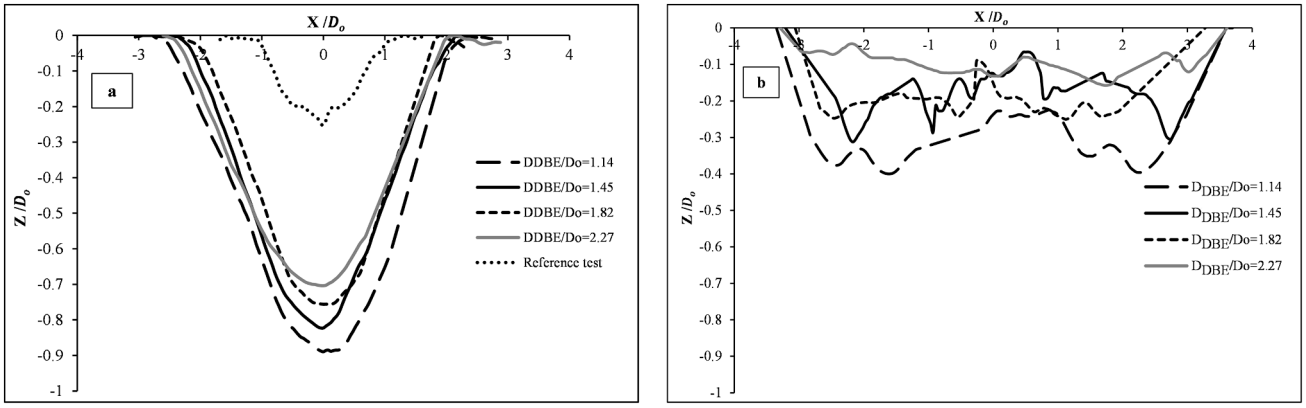


**Fig. 13.** Transverse cross-section of flushing cone in test nos. 45, 46, 47, and 48 for $Y/D_o = 1$ (a) and $Y/D_o = 6.36$ (b).

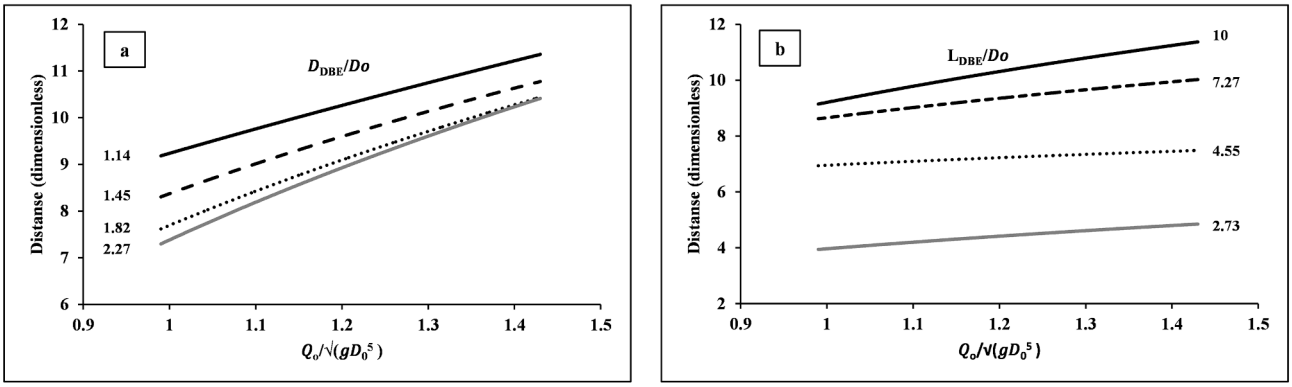


**Fig. 14.** Scour limit vs discharge dimensionless indices for different structure diameter dimensionless indices (a) and different structure length dimensionless indices (b).

between the sediment flushing cone volume dimensionless index and the main variables in Eq. (4), consisting of the DBE length, diameter dimensionless index, and the outflow discharge dimensionless index, with the same constraints as for Eqs. (5)–(7).

$$\frac{V_c}{D_o^3} = 2.887\left(\frac{L_{DBE}}{D_o}\right)^{0.699}\left(\frac{D_{DBE}}{D_o}\right)^{-0.705}(Fr_o)^{1.732} \qquad R^2 = 0.923 \tag{8}$$

Fig. 18 represents the observed values of the sediment flushing cone volume dimensionless index against the values calculated by Eq. (8). According to the results and the standard error (SE) lines representing the average distance of the fall of the observed values below the regression line, the regression line fell between ±5 % SE lines, indicating a cooperative agreement between the experimental and calculated values.

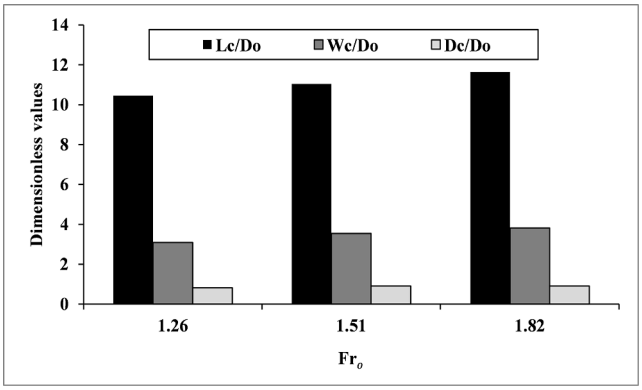


**Fig. 15.** Variations of flushing cone dimensions vs $Fr_o$ indices.

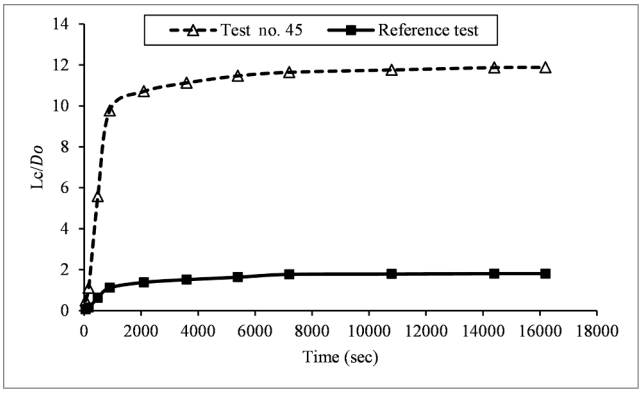


**Fig. 16.** Temporal development of the sediment flushing cone in the reference test compared with test no. 45.

### 3.4. Sediment removal efficiency

The sedimentation efficiency is defined as the ratio of the volume of the sediments to be washed to the volume of water used in the flushing (Haghjouei et al., 2021). The sedimentation efficiency is as follows:

$$E = \frac{\forall_c}{\forall_w} \tag{9}$$

Where $E$ is the flushing efficiency, $\forall_c$ is the sediment volume ($m^3$) evacuated from the reservoir during flushing, and $\forall_w$ is the volume of water ($m^3$) evacuated from the reservoir during flushing.

In this study, the sediment flushing efficiency in test no. 45 was 0.004482 for the dimensionless indices of $L_{DBE}/D_o = 10, D_{DBE}/D_o = 1.14$, and $Fr_o = 1.82$, which indicates an increase of 36.5 times that of the reference.

### 3.5. Comparison between sediment flushing increasing rate of DBE structure with the other structural methods

In this section, the sediment flushing increasing rate of the current study and some structural methods relative to non-structural mode have been compared in Table 4.

The results indicated that DBE structure with optimal diameter and length has a good sediment flushing increasing rate in comparison with other structural methods.

### 3.6. Cost-benefit analysis of using DBE structure

The cost-benefit analysis (CBA) of using the DBE structure for increasing sediment removal efficiency has been illustrated in Table 5. Total costs consist of maintenance and construction cost of using DBE structure, and comprehensive benefits consist of increasing dam reservoir capacity.

## 4. Conclusion

In this research, investigation was carried out on the effect of using recently proposed structure, known as DBE, on the increasing sediment flushing cone dimensions and sediment removal efficiency. The DBE structure enhanced the retrogressive erosion domain, thanks to an expanding velocity profile at the bottom outlet, and increased the sediment flushing cone volume on reservoir various parts due to the creation of a pressure difference between the inside and outside of the structure's branches. Consequently, the use of a DBE structure with the dimensionless index of $L_{DBE}/D_o = 10, D_{DBE}/D_o = 1.14$, and $Fr_o = 1.82$ increased sediment removal efficiency and volume by as much as 36.55 times that of the reference test. It must be mentioned that the findings are applicable for the range of discharges tested. In addition, with an increase in the dimensionless index of length from 2.73 to 10, the length of the maximum increase in the sediment flushing cone reached 6.6 times the reference value, the maximum increase in the width of the sediment flushing cone was equal to 1.75 times the reference value, and the depth of the cone with a constant increase was equal to 1.33 times the reference test value. The results illustrated that an increase in the diameter of the dimensionless index led to maximum variations on the sediment flushing cone dimensions by a minimum dimensionless index of 1.14 because of increased velocity on the minus diameter and consequently the elevated shear stress and its force. Finally, according to a statistical analysis of laboratory data, a dimensionless equation with $R^2 = 0.923$ is presented for the prediction of the sediment flushing cone.

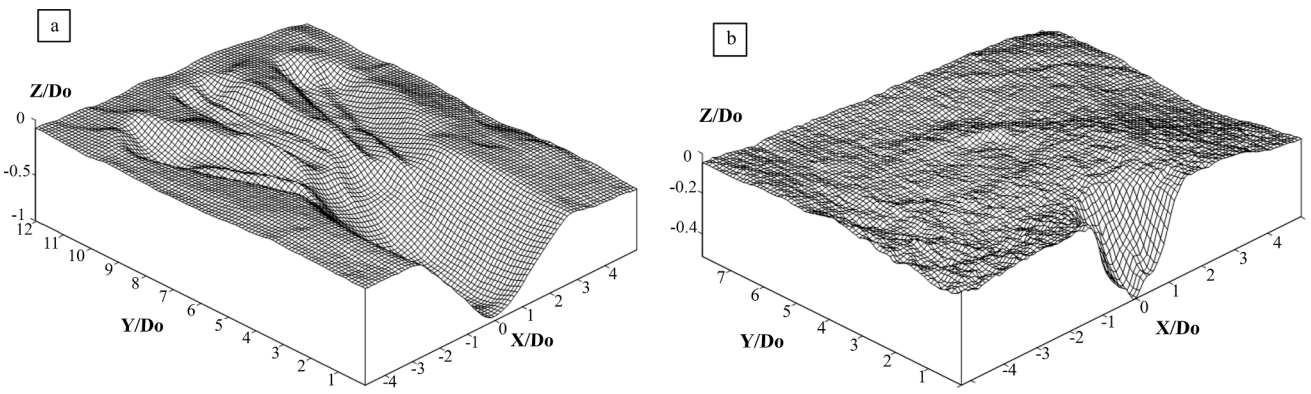


**Fig. 17.** 3D diagram of test no. 45 and reference test (a and b, respectively).

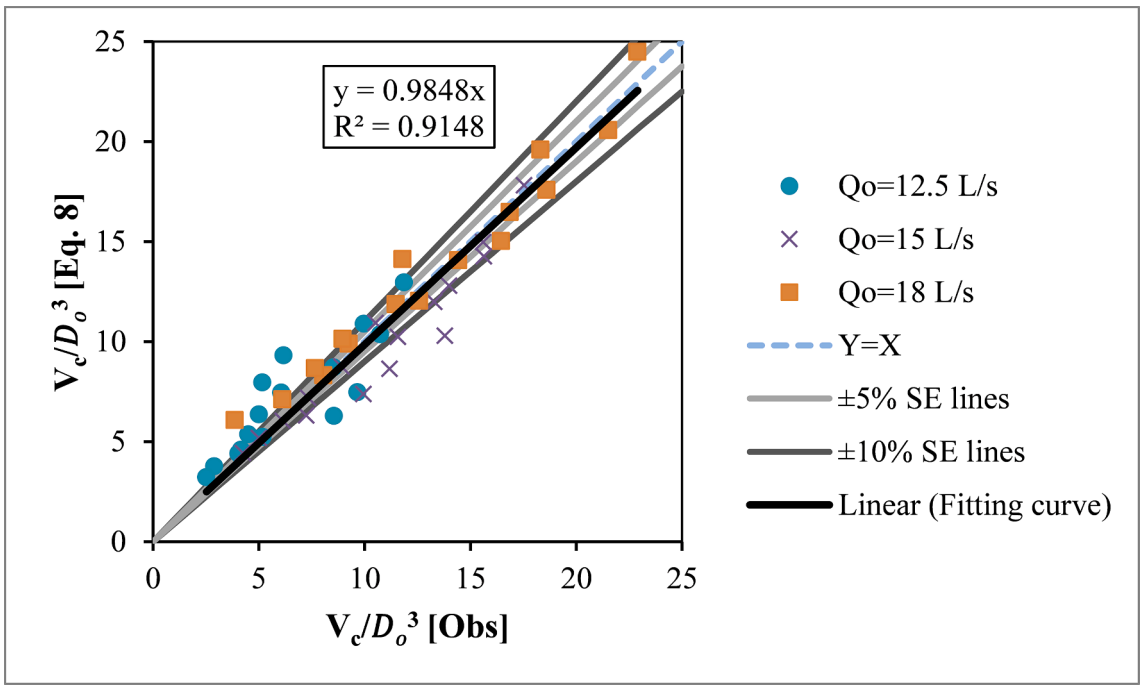


**Fig. 18.** Observed vs calculated sediment flushing cone volume dimensionless index.

**Table 4**
Sediment flushing increasing rate of current study vs some other structural methods.

| Experimental study | Type of structure | Increasing rate relative to the non-structural mode |
|---|---|---|
| Ahadpour Dodaran et al. (2012) | Vibrating Plates | 3.73-fold |
| Althaus et al. (2014) | Water Jet | 2-fold |
| Madadi et al. (2016) | Pile group | 3.5-fold |
| Madadi et al. (2017) | PSC | 4.57-fold |
| Beiramipour et al. (2021) | Submerged Vanes | 48-fold |
| Haghjouei et al. (2021) | DBE | 10-fold |
| The current study | DBE with optimal diameter and length | 36.55-fold |

**Table 5**
CBA results of using DBE structure.

| Total costs of using DBE structure/total cost of the dam | Total benefits of using DBE structure/total cost of the dam | Benefit-cost ratio |
|---|---|---|
| 0.0117 | 0.307 | 26.28 |

## Declaration of Competing Interest

The authors declare that they have no known competing financial interests or personal relationships that could have appeared to influence the work reported in this paper.

## Acknowledgments

This work was supported by JSPS KAKENHI Grant Number JP21H01434.

## References

Ahadpour Dodaran, A., Park, S.K., Mardashti, A., Noshadi, M., 2012. Investigation of dimension changes in under pressure hydraulic sediment flushing cavity of storage dams under effect of localized vibrations in sediment layers. Int. J. Ocean Syst. Eng. 2 (2), 71–81. https://doi.org/10.5574/IJOSE.2012.2.2.071.

Ahn, J., 2011. Numerical modeling of reservoir sedimentation and flushing processes. University of Colorado State. Dissertation.

Ahn, J., Yang, C. T. (2010). Simulation of Xiaolangdi reservoir sedimentation and flushing processes. *2nd joint federal interagency conference*. 27 June–1 July, Las Vegas, NV.

Althaus, J., De Cesare, G., Schleiss, A.J., 2014. Sediment evacuation from reservoirs through intakes by jet-induced flow. J. Hydraul. Eng. (ASCE) 04014078, 1–9. https://doi.org/10.1061/(ASCE)HY.1943-7900.0000970.

Ballio, F., Tait, S., 2012. Sediment transport mechanics. Acta Geophys. J. 60 (6), 1493–1499.

Baoligao, B., Xu, F., Chen, X., Wang, X., Chen, W., 2016. Acute impacts of reservoir sediment flushing on fishes in the Yellow River. J. Hydro-environ. Res. 13, 26–35. https://doi.org/10.1016/j.jher.2015.11.003.

Beiramipour, S., Qaderi, K., Rahimpour, M., Ahmadi, M.M., Kantoush, S.A., 2021. Effect of submerged vanes in front of a circular reservoir intake on sediment flushing cone. Proc. Inst. Civil Eng. Water Manage. 174 (5), 252–266. https://doi.org/10.1680/jwama.20.00032.

Cao, W., Liu, C., & Gu, L. (2019). Reservoir sedimentation management in China. *Hydrolink*, IAHR publishing, Issue 2, 36-39.

Chao, Y.C., Hsieh, T.C., Chen, C.T., Cheng, C.W., Li, H.C., Yeh, K.C., Chen, Y.M., 2021. Impact assessment of reservoir desiltation measure for downstream riverbed migration in climate change: A case study in northern Taiwan. J. Hydro-environ. Res. 37, 67–81. https://doi.org/10.1016/j.jher.2021.05.003.

Dreyer, S. (2018). Investigating the influence of low-level outlet shape on the scour cone formed during pressure flushing of sediments in hydropower plant reservoirs. (M.Sc. thesis). Department of Civil Engineering, University of Stellenbosch, South Africa.

Emamgholizadeh, S., Bina, M., Fathi-Moghadam, M., Ghomeshi, M., 2006. Investigation and evaluation of the pressure flushing through storage reservoir. J. Eng. Appl. Sci. 1 (4), 7–16.

Espa, P., Batalla, R. J., Brignoli, M. L., Crosa, G., Gentili, G., & Quadroni, S. (2019). Tackling reservoir siltation by controlled sediment flushing: Impact on downstream fauna and related management issues. *PLOS ONE*, 14(6), e0218822. https://doi.org/10.1371/journal.pone.0218822.

Gallerano, F., Cannata, G., Lasaponara, F., 2016. Numerical simulation of wave transformation, breaking and run-up by a contravariant fully non-linear Boussinesq equations model. J. Hydrodyn. 28, 379–388. https://doi.org/10.1016/S1001-6058(16)60641-8.

Haghjouei, H., Rahimpour, M., Qaderia, K., Kantoush, S.A., 2021. Experimental study on the effect of bottomless structure in front of a bottom outlet on a sediment flushing cone. Int. J. Sedim. Res. 36 (3), 335–347. https://doi.org/10.1016/j.ijsrc.2020.11.002.

Haun, S., Olsen, N.R.B., 2012. Three-dimensional numerical modeling of the flushing process of the Kali Gandaki hydropower reservoir. Lakes Reservoirs Res. Manage. 17, 25–33. https://doi.org/10.1111/j.1440-1770.2012.00491.x.

Isaac, N., Eldho, T.I., 2016. Sediment management studies of a run-of-the-river hydroelectric project using numerical and physical model simulations. Int. J. River Basin Manage. 14 (2), 165–175. https://doi.org/10.1080/15715124.2015.1105234.

Isaac, N., Eldho, T.I., 2019. Sediment removal from run-of-the-river hydropower reservoirs by hydraulic flushing. Int. J. River Basin Manage. 17 (3), 389–402. https://doi.org/10.1080/15715124.2019.1583667.

Kantoush, S., Suzuki, T., Takemon, Y., El Kadi Abderrezzak, K., Ata, R., Sumi, T., Saber, M. (2018). Numerical study on reservoir sediment management through adding excavated sediment downstream of dams in Japan. Lyon- Villeurbanne, *9th International Conference on Fluvial Hydraulics*, River Flow 2018, Lyon, France. https://doi.org/10.1051/e3sconf/20184003033.

Katano, I., Negishi, J.N., Minagawa, T., Doi, H., Kawaguchi, Y., Kayaba, Y., 2021. Effects of sediment replenishment on riverbed environments and macroinvertebrate assemblages downstream of a dam. Sci. Rep. J. 11, 7525. https://doi.org/10.1038/s41598-021-86278-z.

Kondolf, G.M., Gao, Y., Annandale, G.W., Morris, G.L., Jiang, E., Zhang, J., Cao, Y., Carling, P., Fu, K., Guo, Q., Hotchkiss, R., Peteuil, C., Sumi, T., Wang, H.-W., Wang, Z., Wei, Z., Wu, B., Wu, C., Yang, C.T., 2014. Sustainable sediment management in reservoirs and regulated rivers: Experiences from five continents. Earth's Future 2 (5), 256–280.

Madadi, M.R., Rahimpour, M., Qaderi, K., 2016. Sediment flushing upstream of large orifices: An experimental study. Flow Meas. Instrum. 52, 180–189. https://doi.org/10.1016/j.flowmeasinst.2016.10.007.

Madadi, M.R., Rahimpour, M., Qaderi, K., 2017. Improving the pressurized flushing efficiency in reservoirs: An experimental study. Water Resour. Manage. 31 (14), 4633–4647. https://doi.org/10.1007/s11269-017-1770-y.

Malavoi, J. R., & El Kadi Abderrezzak, K. (2019). Reservoir sedimentation, dam safety and hydropower production: Hazards, risks and issues. *Hydrolink*, IAHR publishing, Issue 2, 50-53.

Meshkati, M.E., Dehghani, A.A., Naser, G., Emamgholizadeh, S., Mosaedi, A., 2009. Evolution of developing flushing cone during the pressurized flushing in reservoir storage. World Acad. Sci. Eng. Technol. 3, 10–27. https://doi.org/10.5281/zenodo.1058207.

Morris, G. L., & Fan, J. (2009). Reservoir Sedimentation Handbook: Design and Management of Dams, Reservoirs, and Watersheds for Sustainable Use; New York, McGraw-Hill, Electronic Version, pp: 784. ISBN: 007043302x / 9780070433021.

Morris, G. L. (2015). Management alternatives to combat reservoir sedimentation. *In Zurich First International Workshop on Sediment Bypass Tunnels*, 181–193. ISSN: 0374-0056.

Powell, D.N., Khan, A.A., 2015. Flow field upstream of an orifice under fixed bed and equilibrium scour conditions. J. Hydraul. Eng. 141 (2) https://doi.org/10.1061/(ASCE)HY.1943-7900.0000960.

Randle, T., Morris. G., Whelan, M., Baker, B., Annandale, G., Hotchkiss, R., … Tullos, D. (2019). Reservoir sediment management: Building a legacy of sustainable water storage reservoirs. *National Reservoir Sedimentation and Sustainability Team White Paper*. Retrieved from: https://www.sedhyd.org/reservoir-sedimentation/National%20Res%20Sed%20White%20Paper%202019-06-21.pdf. Accessed 12 June 2019.

Sawadogo, O., Basson, G.R., Schneiderbauer, S., 2019. Physical and coupled fully three-dimensional numerical modeling of pressurized bottom outlet flushing processes in reservoirs. Int. J. Sedim. Res. 34 (5), 461–474. https://doi.org/10.1016/j.ijsrc.2019.02.001.

Stähly, S., Franca, M.J., Robinson, C.T., Schleiss, A.J., 2019. Sediment replenishment combined with an artificial flood improves river habitats downstream of a dam. Sci. Rep. J. 9, 5176. https://doi.org/10.1038/s41598-019-41575-6.

Sumi, T., & Kantoush, S. A. (2010). Integrated Management of Reservoir Sediment Routing by Flushing, Replenishing, and Bypassing Sediments in Japanese River Basins Dam. *In Proceedings of the 8th International Symposium on Ecohydraulics*, 831–838, Seoul, Korea.

Talebbeydokhti, N., Naghshineh, A., 2004. Flushing sediment through reservoirs. Iran. J. Sci. Technol. Tran. B 28 (B1), 120–136.

Tigrek, S., Gobelez, O., & Aras, T. (2009). Sustainable management of reservoirs and preservation of water quality. 53:41–53. http://om.ciheam.org/article.php?IDPDF=801179.

Trimble, S.W., Wilson, B., Herschy, R., Dargahi, B., Chanson, H., Herschy, R.W., Saltankin, V.P., 2012. Reservoir and lake trap efficiency. In: Bengtsson, L., Herschy, R.W., Fairbridge, R.W. (Eds.), Encyclopedia of Lakes and Reservoirs. Encyclopedia of Earth Sciences Series. Springer, Dordrecht, pp. 628–649.

White, W. R., & Bettess, R. (1984). The feasibility of flushing sediments through reservoirs. *In Proceedings of the Harare Symposium*, July 1984, Harare. IAHS Publication No. 144, pp. 577–587.

White, R. (2001). *Evacuation of sediments from reservoirs*, London: Thomas Telford Publishing. https://doi.org/10.1680/eosfr.29538.